Cellular and Molecular Biology
E-ISSN : 1165-158X / P-ISSN : 0145-5680
www.cellmolbiol.org

# Molecular interaction of cryptophycin 52 with Caspase 8 for the management of lung cancer during coronavirus outbreak: A computational study

Leena Hussein Bajrai[1,2], Sayed Sartaj Sohrab[1,3], Mohammad Khalid[4], Mohammad A. Kamal[1,5,6,7], Esam Ibraheem Azhar[1,2*]

[1] Special Infectious Agents Unit, King Fahd Medical Research Centre, King Abdulaziz University, Jeddah, Saudi Arabia.
[2] Biochemistry Department, Faculty of Sciences, King Abdulaziz University, Jeddah, Saudi Arabia
[3] Medical Laboratory Sciences Department, Faculty of Applied Medical Sciences, King Abdulaziz University, Jeddah, Saudi Arabia
[4] Department of Pharmacognosy, College of Pharmacy, Prince Sattam Bin Abdulaziz University, P.O. Box 173, Al-Kharj 11942, Saudi Arabia
[5] West China School of Nursing / Institutes for Systems Genetics, Frontiers Science Center for Disease-related Molecular Network, West China Hospital, Sichuan University, Chengdu 610041, Sichuan, China
[6] Department of Pharmacy, Faculty of Allied Health Sciences, Daffodil International University, Bangladesh
[7] Enzymoics, NSW; Novel Global Community Educational Foundation, Australia

**ARTICLE INFO**

***Original paper***

***Article history:***
*Received: January 18, 2022*
*Accepted: March 12, 2022*
*Published: June 30, 2022*

***Keywords:***

*AutoDock, Binding energy, Lung cancer, Casp8, COVID-19 outbreak, MD simulations.*

**ABSTRACT**

It has been seen that, during COVID-19 outbreak lung cancer (LC) patients are noted as a high-risk population which make a more challenging to treatment of the LC patients. The active form of caspase-8 is involved in lung carcinogenesis in both humans and mice. In this study, the virtual screening was performed among 200 compounds retrieved from several resources for the searching of potent lead against Caspase 8 (Casp8). Cryptophycin 52 was found to have a strong inhibiting efficacy based on the free energy of binding with the active site of Casp8. The lowest binding energy was found to be -8.05 kcal/mole and was further analyzed for molecular dynamic simulation. Casp8 enzyme was determined to interact with cryptophycin 52 through twelve amino acid residues, specifically ARG260, SER316, GLY318, ASP319, THR337, VAL354, PHE355, PHE356, ILE357, GLN358, ALA359 and CYS360 along with six hydrogen bond particular, ILE357:N-UNK1: O7, UNK1: O14-PHE355:O, UNK1: C25-PHE355:O, UNK1: C35-THR337:O, UNK1: H65-HE355:O and UNK1: C25-PHE356. In addition, MD simulations for 50ns were performed for optimization, flexibility estimation and assessment of Casp8-cryptophycin 52 complex stability. This complex was seen as reasonably stable according to the RMSD, RMSF, and radius of gyration graph. Results obtained indicate cryptophycin 52 may be a lead compound with significant anti-cancer ability against Casp8. Further experimental work, however, is expected to support the compound's anti-cancer viewpoint.

**Doi:** http://dx.doi.org/10.14715/cmb/2022.68.6.5 

## Introduction

The novel coronavirus infection was announced in late December 2019 (1-3). It is a big pandemic caused by SARS-CoV-2 in the world (4). Due to the high rate of spreading across the globe, it has been placed in class B infectious disease. It has been seen that, during the COVID-19 outbreak, lung cancer (LC) patients are noted as a high-risk population which makes it more challenging to the treatment of LC patients. It is also a great challenge to differentiate the LC patients with COVID-19 in terms of clinical symptoms (5). Due to the spread of COVID-19, the monotonous medical diagnosis and treatment for LC patients have been disturbed. LC patients should be the main concern group for COVID-19 hindrance (6). It is vital to select accessible medications that can suppress or prevent the sickness due to the emergency and uncontrollable scenario produced by the COVID-19 pandemic that has spread over the whole planet. Despite the quicker development of vaccinations, there is still a need for medications to combat the SARS CoV-2(7-9).

Mouse hepatitis virus (MHV) is a prototype of murine coronavirus. Casp8 activation was observed in MHV-infected 17Cl-1 cells (2). The use of a pan-caspase inhibitor resulted in the inhibition of SADS-CoV-induced apoptosis and decline in Swine acute diarrhea syndrome coronavirus (SADS-CoV) replication, indicative of the relationship of a caspase-dependent pathway. Furthermore, SADS-CoV infection activated the initiators Casp8 and 9 and upregulated FasL and Bid cleavage, indicating crosstalk between the extrinsic and intrinsic pathways (10).

LC is the most crucial reason for death globally. LC is mainly linked with cigarette smoking (11, 12). It is the most common of all cancer forms worldwide, with 1.8 million people diagnosed per year, resulting in 1.6 million deaths annually as per the American cancer society (13). LC has been converted from a rare disease to a major public health issue. LC's etiology becomes more challenging with industrialization, urbanization and environmental degradation all over the world. LC treatment/control has currently attracted worldwide attention (14). Different caspases are involved in apoptosis-mediated cell death.

* Corresponding author. Email: eazhar@kau.edu.sa

Apoptosis-mediated cell death involves various caspases. Indeed, Casp8 is one of the upstream cell death mediators and its activation is related to an increase of TNF-like cytokines, such as TNF-α and Fas ligand (15). The appearance of Casp8 in the LC tissues was noticed by immunohistochemistry. The expression of Casp8 was found in 38/52 cancer tissues, 22/30 neighboring tissues, and 34/52 normal tissues. The tissue number of Casp8 positive expression in different groups was similar, but the intensity of Casp8 expression in different groups was statistically dissimilar (16). Automated cell death, which is based on caspases, is commonly called apoptosis, while caspase-1 is involved in the activation of an inflammation allied with programmed cell death, defined as pyroptosis (17). Two major pathways to apoptosis have been identified, 'intrinsic' and 'extrinsic.' Caspase-9 initiates intrinsic apoptosis (18). Extrinsic apoptosis occurs after death signaling and is triggered by Casp8 and 10 (19). Terlizzi et al. (2015) Demonstrate that active Casp8 is concerned in LC in humans and mice (20). The numerous compounds have been reported to have many biological activities as anti-cancer (21). The compounds and their derivatives mimic over 50% of all drugs that are being used clinically (22). The present work aimed in silico investigation of inhibitors against Casp8 from different sources. The hit compounds obtained from this study could play an important role in designing personalized therapy against LC patients and innovative drug discoveries against Casp8. In this study, the virtual screening process was performed in the search for the best lead against Casp8. Cryptophycin-52 was found to be a good inhibiting efficiency based on the free energy of binding against Casp8. Cryptophycin 52 is a member of the antitumor agent family of cryptophycins currently undergoing clinical trials for cancer chemotherapy assessment (23). A wide variety of antitumor activity has been demonstrated against xenografts of human tumors and murine tumors. Its mechanism of action includes the arrest and suppression of cells during the G2-M phase of the cell cycle by binding to microtubules and their dynamics (24). Cryptophycin 52 is a promising anti-tubulin drug with efficacy in non-small cell lung cancer recognized in vitro and in vivo (25). The study focuses on virtual screening of compounds that bears anticancer potential and thus, inhibiting Casp8 using a computational approach. This study was successfully conducted to anticipate the function of screened compound Cryptophycin 52, that is known to bear anticancer property.

## Materials and Methods

### Preparation of target structure

RCSB Protein Data Bank was used to acquire the 3D structure of the enzyme (PDB ID-1QTN) for docking analysis. The PDB structure has been cleaned and heteroatoms of the protein have been eliminated as these are non-standard deposits of the target molecules.

### Preparation of ligand structures

The SMILES representation of the cryptophycin 52 was obtained from the PubChem database of NCBI (https://pubchem.ncbi.nlm.nih.gov/). The 3D structure was built by utilizing the online web tools CORINA (http://www.molecular-networks.com/products/Corina).

### Molecular docking simulations

Autodock 4.2 was used for docking analysis (26) in this study. A virtual docking study was conducted to determine how the structures of compound cryptophycin 52 contribute to their inhibitory activity against Casp8. The Docking system included the preparation of receptor and ligand molecules. All docking parameters have been kept as standard.

### Grid parameters file

The grids were sketched as such that the ligand was permitted to rotate uninhibitedly inside the grid point. A lattice of 60 Å × 60 Å × 60 Å with 0.375 Å dispersing was outlined through "Auto grid" aimed to target the binding pocket of the receptors.

### Docking parameter file

For the preparation of dpf file, the genetic algorithm "Number of genetic algorithm runs", "Crossover frequency" and "Mutation rates" were set to default standards. Lamarckian Genetic Algorithm (LGA) was adopted in receptor and ligand for flexible docking computation. The conformer with the lowest free energy of binding was considered for further analysis (27, 28).

### Visualization of complex structure

Eventually, the interactions were analyzed in terms of binding energy and inhibition constant in consort with the number of H-bonds with the amino acid residues. The figures of the best-docked arrangements of the ligand and receptor complex were produced utilizing the Discovery Studio Visualizer.

### MD Simulation study

For the analysis of stability and flexibility of the 'Casp8 - cryptophycin 52' complex, MD simulation was done using GROMACS 5.1.4 suite (29). ProDRG server was applied for the preparation of cryptophycin 52 topology files (30). The complex (Casp8- cryptophycin 52)was solvated in 377.187 $nm^3$ cubic box. The steepest descent algorithm for 50,000 steps with a cut-off value up to 1000 $kJmol^{-1}$ was applied for energy minimization. Further, the LINCS algorithm (31) was used for covalent bond constraints. NVT (constant number of particles, Volume, Temperature) and NPT (constant number of particles, pressure, and temperature) phase of equilibration was executed at 300 K with the Berendsen pressure coupling process (32). MD simulation was carried out for 50 ns. MD simulation outcomes like RMSD, RMSF, and radius of gyration of 'Casp8- cryptophycin 52' complex was analyzed.

## Results and discussion

Apoptosis is a genetically regulated mechanism for cell death that plays a crucial role in several physiological processes and in maintaining tissue homeostasis (33-35). Casp8 plays a crucial function in the central apoptotic pathway involving ligands and their receptors that cause death (36, 37). Chief initiator caspase activation (Casp8) turns on the downstream executioner (effector) caspases, the key being Casp3, which coordinates the apoptosis execution phase by cleaving multiple structural and repair proteins (38). Furthermore, the pharmacological inhibition of Casp8 has been demonstrated to have an anti-tumor

effect and is novel evidence not only of the involvement of Casp8 in LC but also of the involvement of the inflammasome in this context (20).

Here in this study, a library of 200 compounds from several resources was prepared and subjected to virtual screening through molecular docking against the Casp8 utilizing the AutoDock tool. Finally, based on the free energy of binding, Cryptophycin 52 was found the best, which was further proceeded for MD simulation analysis. It is worth observing that both the 'ligand' and the 'protein side chains' were held flexible throughout the study by the docking software (39). Protein-ligand interaction is an indispensable focus in the receptor-based drug design and prediction of protein function. Molecular docking, as well as molecular dynamic (MD) simulations, are broadly accepted methods to predict the binding modes and affinities and steadiness of the diverse protein-ligand interactions (40). In-depth docking study was conducted on Cryptophycin 52 with Casp8. The Casp8 enzyme was identified as interacting with cryptophycin 52 through 12 amino acid residues, namely ARG260, SER316, GLY318, ASP319, THR337, VAL354, PHE355, PHE356, ILE357, GLN358, ALA359 and CYS360. The binding energy and inhibition constant for this complex were found to be -8.05 kcal/mole and 287.51µmol, respectively. It is stated that a higher (negative) free energy of binding values obtained using computational studies can recommend only the binding efficiency for an enzyme and ligand interaction (41). Four amino acid residues like THR337, PHE355, PHE356 and ILE357 were involved in six H-bond formations in the correct positioning of Cryptophycin 52 interaction with Casp8, namely ILE357:N-UNK1:O7, UNK1:O14-PHE355:O, UNK1:C25-PHE355:O, UNK1:C35-THR337:O, UNK1:H65-HE355:O and UNK1:C25-PHE356 along with H-bond distances 2.731155, 2.653552, 2.809291, 2.848232, 2.907828, and 3.484625 Å respectively shown in Figure 1.

It has been recognized that the H-bonds formed between the compound and the protein most frequently contribute to the stabilization of the protein-ligand complex, with various hydrogen bonds responsible for the stability of the complex (42, 43). Three hydrophobic interaction was found to be involved in this complex formation. C23, C24 and C26 of ligand molecule were found to interact with VAL35 of the receptor. 'Van der Waals', 'H-bond' and 'Desolvation' energy components together contributed -7.01 kcal/mol for 'Cryptophycin 52- Casp8 complex'. For this complex, the 'Electrostatic' energy was found to be -0.01 kcal/mol. The total interacting surface area for the interacting complex was found to be 658.558Å$^2$. The thermodynamic data (44) was also attained through molecular docking interactions analysis, including free energy, internal energy and entropy at a constant temperature, 298.15K. Free energy and internal energy values were found to be -1368.17 and -3.94 kcal/mol, respectively, while entropy was estimated as 4.58 kcal/mol/K for this complex interaction.

This docked complex was directed to MD simulation to validate the stability of the interaction between cryptophycin 52 and Casp8. The time-dependent performance of MD trajectories was examined in terms of root mean square deviation (RMSD), root mean square fluctuation (RMSF), and radius of gyration (Rg) for all backbone atoms. The RMSD is an important constraint in evaluating the equilibration of MD trajectories (45). The RMSD of the Casp8 backbone atoms was developed as a function of time to monitor the complex's stability in MD. RMSD graph shows that the complex of Casp8 and cryptophycin 52 is stable and less flexible. The complex achieved equilibrium in the initial simulation process and then remained stable throughout the 50 ns period as seen in Figure 2.

RMSF is a significant parameter that yields data about the structural adaptability of Cα atoms of every residue in the corresponding framework (46). RMSF for every residue of Casp8 complexes with cryptophycin 52 was examined, as appears in Figure 3. The active residues of Casp8 associated with cryptophycin 52 have not indicated fundamentally fluctuation.

The radius of gyration (Rg) is utilized to clarify the stability of enzyme -ligand complex. It is characterized as the mass-weighted root mean square distance of an assortment of atoms from their regular center of mass. Analysis of Rg gives us knowledge of the overall dimensions of the protein (47).

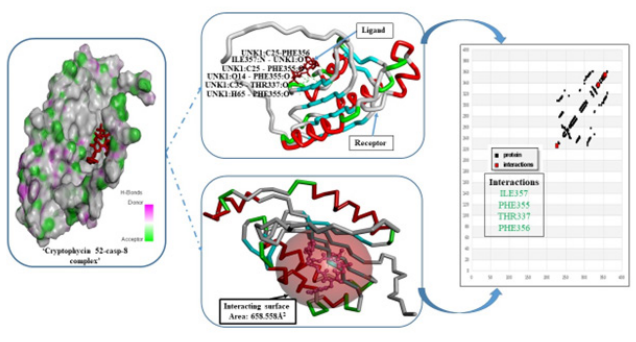


**Figure 1.** Docked structure of lowest-energy for the Casp8/ Cryptophycin 52 complex.

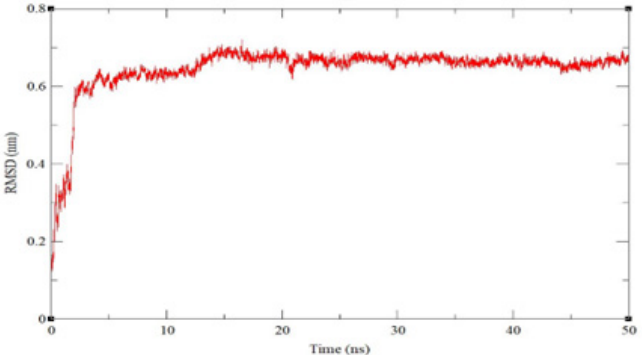


**Figure 2.** The root means square deviation of Casp8/ Cryptophycin 52 complex obtained by MD simulation.

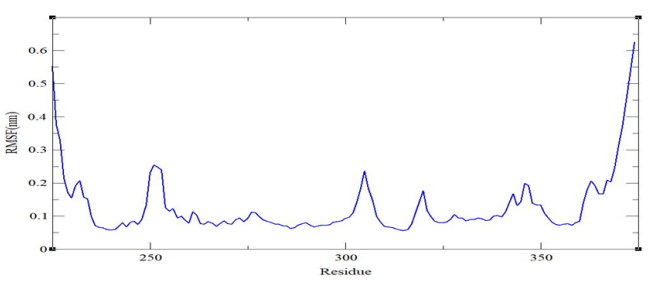


**Figure 3.** The root mean square fluctuation of the Casp8/ Cryptophycin 52 complex .

The value of Rg for the protein backbone was determined for 50 ns trajectory and shown in Figure 4. Rg results recommend that the complex was stable and the secondary structures of the protein are compactly packed in the simulation.

The study focuses on virtual screening of compounds that bears anticancer potential and thus, inhibiting casp-8 using a computational approach. The virtual screened compound displays a better inhibition efficiency against Casp8. The presence of numerous H-bond and hydrophobic interactions were observed in the binding affinity of the compound to the receptor structure and helped into the correct positioning compound to the active site of Casp8. The complex achieved equilibrium in the initial simulation process and then remained stable throughout the 50 ns period. This data confirms that the ligand was effective inhibitor of Casp8 based on their binding energy and dynamics simulation study.

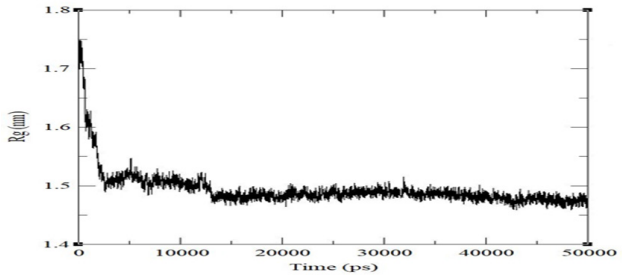


**Figure 4.** Radius of gyration of Cryptophycin 52 against Casp8.

## Consent for Publication

Not applicable.

## Conflict of Interest

The authors declare no conflict of interest.

## Acknowledgments

The Deanship of Scientific Research (DSR) at King Abdulaziz University, Jeddah, Saudi Arabia funded this project, under grant no. (FP-100-42).

## References

1. Ludwig S, Zarbock A. Coronaviruses and SARS-CoV-2: A Brief Overview. Anesth Analg. 2020;131(1):93-6. doi: 10.1213/ANE.0000000000004845.
2. Chen CJ, Makino S. Murine coronavirus-induced apoptosis in 17Cl-1 cells involves a mitochondria-mediated pathway and its downstream caspase-8 activation and bid cleavage. Virology. 2002;302(2):321-32. doi: 10.1006/viro.2002.1626.
3. Alebouyeh M, Aavani P, Abdulrahman NA, Haleem AA, Karimi A, Armin S, et al. Re-positive PCR of SARS-CoV-2 in health care persons during COVID-19 pandemic. Cell Mol Biol (Noisy-le-grand). 2022;67(5):138-43. doi: 10.14715/cmb/2021.67.5.19.
4. Dhar D, Mohanty A. Gut microbiota and Covid-19- possible link and implications. Virus Res. 2020;285:198018. doi: 10.1016/j.virusres.2020.198018.
5. Yang L, Xu HY, Wang Y. [Diagnostic and therapeutic strategies of lung cancer patients during the outbreak of 2019 novel coronavirus disease (COVID-19)]. Zhonghua Zhong Liu Za Zhi. 2020;42(4):292-5. doi: 10.3760/cma.j.cn112152-20200229-00152.
6. Xu Y, Liu H, Hu K, Wang M. [Clinical Management of Lung Cancer Patients during the Outbreak of 2019 Novel Coronavirus Disease (COVID-19)]. Zhongguo Fei Ai Za Zhi. 2020;23(3):136-41. doi: 10.3779/j.issn.1009-3419.2020.03.02.
7. Adel K, Amor M, Alaeddine R, Emira N, Mousa A, Kaiss A, et al. Comparative Computational Analysis of Dirithromycin and Azithromycin in Search for a Potent Drug against COVID-19 caused by SARS-CoV-2: Evidence from molecular docking and dynamic simulation. Cell Mol Biol (Noisy-le-grand). 2022;67(5):371-86. doi: 10.14715/cmb/2021.67.5.50.
8. Zrieq R, Snoussi M, Algahtan FD, Tasleem M, Saeed M, Noumi E, et al. Repurposing of anisomycin and oleandomycin as a potential anti-(SARS-CoV-2) virus targeting key enzymes using virtual computational approaches. Cell Mol Biol (Noisy-le-grand). 2022;67(5):387-98. doi: 10.14715/cmb/2021.67.5.51.
9. Snoussi M, Noumi E, Mosbah A, Redissi A, Saeed M, Tasleem M, et al. Tripeptides from Allium subhirsitum L. extracts: Pharmacokinetics properties, toxicity prediction and in silico study against SARS-CoV-2 enzymes and pro-inflammatory proteins. Cell Mol Biol (Noisy-le-grand). 2022;67(4):143-62. doi: 10.14715/cmb/2021.67.4.17.
10. Zhang J, Han Y, Shi H, Chen J, Zhang X, Wang X, et al. Swine acute diarrhea syndrome coronavirus-induced apoptosis is caspase- and cyclophilin D- dependent. Emerg Microbes Infect. 2020;9(1):439-56. doi: 10.1080/22221751.2020.1722758.
11. Romaszko AM, Doboszynska A. Multiple primary lung cancer: A literature review. Adv Clin Exp Med. 2018;27(5):725-30. doi: 10.17219/acem/68631.
12. Rivera GA, Wakelee H. Lung Cancer in Never Smokers. Adv Exp Med Biol. 2016;893:43-57. doi: 10.1007/978-3-319-24223-1_3.
13. Sharda S, Khandelwal R, Adhikary R, Sharma D, Majhi M, Hussain T, et al. A Computer - Aided Drug Designing for Pharmacological Inhibition of Mutant ALK for the Treatment of Non-small Cell Lung Cancer. Curr Top Med Chem. 2019;19(13):1129-44. doi: 10.2174/1568026619666190521084941.
14. Mao Y, Yang D, He J, Krasna MJ. Epidemiology of Lung Cancer. Surg Oncol Clin N Am. 2016;25(3):439-45. doi: 10.1016/j.soc.2016.02.001.
15. Blander JM. A long-awaited merger of the pathways mediating host defence and programmed cell death. Nat Rev Immunol. 2014;14(9):601-18. doi: 10.1038/nri3720.
16. Du N, Sun XF, Hu LJ, Sun X, Li XJ, Zhao Y, et al. [Expression of caspase-8 in non-small cell lung cancer and its role in invasion and metastasis of lung cancer A549 cells]. Xi Bao Yu Fen Zi Mian Yi Xue Za Zhi. 2012;28(6):572-5.
17. Kroemer G, Galluzzi L, Vandenabeele P, Abrams J, Alnemri ES, Baehrecke EH, et al. Classification of cell death: recommendations of the Nomenclature Committee on Cell Death 2009. Cell Death Differ. 2009;16(1):3-11. doi: 10.1038/cdd.2008.150.
18. Lindsay J, Esposti MD, Gilmore AP. Bcl-2 proteins and mitochondria--specificity in membrane targeting for death. Biochim Biophys Acta. 2011;1813(4):532-9. doi: 10.1016/j.bbamcr.2010.10.017.
19. Kantari C, Walczak H. Caspase-8 and bid: caught in the act between death receptors and mitochondria. Biochim Biophys Acta. 2011;1813(4):558-63. doi: 10.1016/j.bbamcr.2011.01.026.
20. Terlizzi M, Di Crescenzo VG, Perillo G, Galderisi A, Pinto A, Sorrentino R. Pharmacological inhibition of caspase-8 limits lung tumour outgrowth. Br J Pharmacol. 2015;172(15):3917-28. doi: 10.1111/bph.13176.
21. Harvey AL. Natural products in drug discovery. Drug Discov Today. 2008;13(19-20):894-901. doi: 10.1016/j.drudis.2008.07.004.
22. Nand M, Maiti P, Pant R, Kumari M, Chandra S, Pande V. Virtual screening of natural compounds as inhibitors of EGFR 696-1022 T790M associated with non-small cell lung cancer. Bioinforma-

tion. 2016;12(6):311-7. doi: 10.6026/97320630012311.
23. Wagner MM, Paul DC, Shih C, Jordan MA, Wilson L, Williams DC. In vitro pharmacology of cryptophycin 52 (LY355703) in human tumor cell lines. Cancer Chemother Pharmacol. 1999;43(2):115-25. doi: 10.1007/s002800050871.
24. Al-Awar RS, Corbett TH, Ray JE, Polin L, Kennedy JH, Wagner MM, et al. Biological evaluation of cryptophycin 52 fragment A analogues: effect of the multidrug resistance ATP binding cassette transporters on antitumor activity. 2004;3(9):1061-7.
25. Edelman MJ, Gandara DR, Hausner P, Israel V, Thornton D, DeSanto J, et al. Phase 2 study of cryptophycin 52 (LY355703) in patients previously treated with platinum based chemotherapy for advanced non-small cell lung cancer. Lung Cancer. 2003;39(2):197-9. doi: 10.1016/s0169-5002(02)00511-1.
26. Goodsell DS, Morris GM, Olson AJ. Automated docking of flexible ligands: applications of AutoDock. J Mol Recognit. 1996;9(1):1-5. doi: 10.1002/(sici)1099-1352(199601)9:1<1::aid-jmr241>3.0.co;2-6.
27. Rehman A, Akhtar S, Siddiqui MH, Sayeed U, Ahmad SS, Arif JM, et al. Identification of potential leads against 4-hydroxytetrahydrodipicolinate synthase from Mycobacterium tuberculosis. Bioinformation. 2016;12(11):400-7. doi: 10.6026/97320630012400.
28. Sharma N, Akhtar S, Jamal QMS, Kamal MA, Khan MKA, Siddiqui MH, et al. Elucidation of Antiangiogenic Potential of Vitexin Obtained from Cucumis sativus Targeting Hsp90 Protein: A Novel Multipathway Targeted Approach to Restrain Angiogenic Phenomena. Med Chem. 2017;13(3):282-91. doi: 10.2174/1573406413666161111152720.
29. Abraham MJ, Murtola T, Schulz R, Páll S, Smith JC, Hess B, et al. GROMACS: High performance molecular simulations through multi-level parallelism from laptops to supercomputers. SoftwareX. 2015;1:19-25.
30. Schuttelkopf AW, van Aalten DM. PRODRG: a tool for high-throughput crystallography of protein-ligand complexes. Acta Crystallogr D Biol Crystallogr. 2004;60(Pt 8):1355-63. doi: 10.1107/S0907444904011679.
31. Hess B, Bekker H, Berendsen HJ, Fraaije JG. LINCS: a linear constraint solver for molecular simulations. Journal of computational chemistry. 1997;18(12):1463-72.
32. Agrahari AK, Doss GPC, Siva R, Magesh R, Zayed H. Molecular insights of the G2019S substitution in LRRK2 kinase domain associated with Parkinson's disease: A molecular dynamics simulation approach. J Theor Biol. 2019;469:163-71. doi: 10.1016/j.jtbi.2019.03.003.
33. Golstein P. Controlling cell death. Science. 1997;275(5303):1081-2. doi: 10.1126/science.275.5303.1081.
34. Cryns V, Yuan J. Proteases to die for. Genes Dev. 1998;12(11):1551-70. doi: 10.1101/gad.12.11.1551.
35. Wyllie AH. Apoptosis: an overview. Br Med Bull. 1997;53(3):451-65. doi: 10.1093/oxfordjournals.bmb.a011623.
36. Ashkenazi A, Dixit VM. Apoptosis control by death and decoy receptors. Curr Opin Cell Biol. 1999;11(2):255-60. doi: 10.1016/s0955-0674(99)80034-9.
37. Schneider P, Tschopp J. Apoptosis induced by death receptors. Pharm Acta Helv. 2000;74(2-3):281-6. doi: 10.1016/s0031-6865(99)00038-2.
38. Slee EA, Adrain C, Martin SJ. Executioner caspase-3, -6, and -7 perform distinct, non-redundant roles during the demolition phase of apoptosis. J Biol Chem. 2001;276(10):7320-6. doi: 10.1074/jbc.M008363200.
39. Shaikh S, Ahmad SS, Ansari MA, Shakil S, Rizvi SM, Shakil S, et al. Prediction of comparative inhibition efficiency for a novel natural ligand, galangin against human brain acetylcholinesterase, butyrylcholinesterase and 5-lipoxygenase: a neuroinformatics study. CNS Neurol Disord Drug Targets. 2014;13(3):452-9. doi: 10.2174/18715273113126660162.
40. Naqvi AAT, Mohammad T, Hasan GM, Hassan MI. Advancements in Docking and Molecular Dynamics Simulations Towards Ligand-receptor Interactions and Structure-function Relationships. Curr Top Med Chem. 2018;18(20):1755-68. doi: 10.2174/1568026618666181025114157.
41. Alam A, Shaikh S, Ahmad SS, Ansari MA, Shakil S, Rizvi SM, et al. Molecular interaction of human brain acetylcholinesterase with a natural inhibitor huperzine-B: an enzoinformatics approach. CNS Neurol Disord Drug Targets. 2014;13(3):487-90. doi: 10.2174/18715273113126660163.
42. Steiner T, Koellner G. Hydrogen bonds with pi-acceptors in proteins: frequencies and role in stabilizing local 3D structures. J Mol Biol. 2001;305(3):535-57. doi: 10.1006/jmbi.2000.4301.
43. Weiss MS, Brandl M, Suhnel J, Pal D, Hilgenfeld R. More hydrogen bonds for the (structural) biologist. Trends Biochem Sci. 2001;26(9):521-3. doi: 10.1016/s0968-0004(01)01935-1.
44. Cappel D, Sherman W, Beuming T. Calculating Water Thermodynamics in the Binding Site of Proteins - Applications of WaterMap to Drug Discovery. Curr Top Med Chem. 2017;17(23):2586-98. doi: 10.2174/1568026617666170414141452.
45. Sharma N, Sharma M, Shakeel E, Jamal QMS, Kamal MA, Sayeed U, et al. Molecular Interaction and Computational Analytical Studies of Pinocembrin for its Antiangiogenic Potential Targeting VEGFR-2: A Persuader of Metastasis. Med Chem. 2018;14(6):626-40. doi: 10.2174/1573406414666180416125121.
46. Ul Haq F, Abro A, Raza S, Liedl KR, Azam SS. Molecular dynamics simulation studies of novel beta-lactamase inhibitor. J Mol Graph Model. 2017;74:143-52. doi: 10.1016/j.jmgm.2017.03.002.
47. Baig MH, Sudhakar DR, Kalaiarasan P, Subbarao N, Wadhawa G, Lohani M, et al. Insight into the effect of inhibitor resistant S130G mutant on physico-chemical properties of SHV type beta-lactamase: a molecular dynamics study. PLoS One. 2014;9(12):e112456. doi: 10.1371/journal.pone.0112456.